Int. J. Electrochem. Sci., 3 **(2008)** 676 - 690

International Journal of
ELECTROCHEMICAL
SCIENCE
www.electrochemsci.org

Inverse Method Applied for the Determination of the Wall Shear Rate in a Scraped Surface Heat Exchanger using the Electrochemical Technique

F. Aloui [1,3,*], *F. Rehimi* [2], *E. Dumont* [3], *J. Legrand* [4]

[1] Université de Nantes – Faculté des Sciences et des Techniques. Département de Physique, Laboratoire GEPEA - UMR CNRS 6144, 2, rue de la Houssinière BP 92208 44322 Nantes Cedex 03 – France
[2] Université de Monastir, École Nationale d'Ingénieurs de Monastir, Laboratoire LESTE, Avenue Ibn El Jazzar 5019, Monastir, Tunisie
[3] École des Mines de Nantes, Département des Systèmes Énergétiques et Environnement (DSEE),Laboratoire GEPEA - UMR CNRS 6144, rue Alfred Kastler - la Chantrerie, BP 20722, 44307 Nantes Cedex 03
[4] CRTT - GEPEA - CNRS-UMR 6144 - Boulevard de l'Université - BP 406 ; 44602 Saint-Nazaire Cedex (France)
[*]E-mail: fethi.aloui@univ-nantes.fr

Received: 27 February 2008 / *Accepted:* 14 March 2008 / *Online published:* 20 April 2008

In this study, an inverse method is presented so as to determine the wall shear rate in a scraped surface heat exchanger using polarography technique. Based on a numerical sequential estimation, this method which enables the inversion of the convection diffusion equation, is applied to measured mass transfer temporal signals. Other solutions, mostly used in polarograghy, are also presented in order to compare them with this inverse technique; they are the quasi-steady (Levêque) and the Sobolik et al. methods. The objective of this study is to understand the validity limits of these classical methods, and to frame their uses in mass transfer studies. The experimental device used is an industrial scraped surface heat exchanger with a high viscous of an isotherm Newtonian or non Newtonian liquid, normally utilized in food engineering. Three liquid solutions have been in main used in this test setup: Emkarox HV45 (which is a mixture of polypropylene glycol and polyethylene glycol), a low viscous Newtonian solution of polyethylene glycol 35000 (PEG), and a shear-thinning guar gum solution (where the rheological behaviour was modelled by two different power-laws according to the shear rate domains). That is why the determination of the "true" wall shear rate is primordial.

Keywords: Inverse Method; sequential estimation; scraped surface heat exchanger; mass transfer; wall shear stress; electrochemical method

1. INTRODUCTION

Electrochemical method is widely used to measure wall shear rate in order to study various hydrodynamic problems. Hence, the well-known Taylor-Couette flow has often been studied using circular probes in order to clearly understand the nature of the transition between laminar flow and fully developed turbulent flow (Kataoka et al., 1977; Legrand et al., 1983; Wronsky and Jastrzebski, 1990). These studies devoted to annular gaps are of particular significance because their geometry is the basis of a variety of technical apparatuses, such as the scraped surface heat exchanger (SSHE). This latter, widely spread in the food industry, allows highly viscous fluids with complex rheology to be processed (cream cheese, fruit concentrate, ice cream, among others); and its specificity lies in the rotation of a shaft equipped with blades that periodically scrape the exchange surface in order to prevent crust formation and to promote heat transfer (Fig. 1a). As for continuous processes, an axial flow is added, so that the flow pattern is a superposition of a Poiseuille flow in an annular space and a Couette flow, to which perturbations created by the blades are added. In previous works (Dumont et al., 2000a, b) we have successfully demonstrated that electrochemical technique could be used to measure wall shear rate in a scale-down model of SSHE with highly viscous solutions. Laminar and vortex flow regimes were investigated and compared to flow regimes in annulus space. Unlike wall shear rates in an annulus which depends on the flow regime, our results showed that the shear rate on the stator wall of a SSHE is controlled by blades rotation. In this case, the maximum values of the wall shear rates appear 10-100 times higher than those in an annulus space without blades. Previous work (Dumont et al., 2000a) also indicated that in a specific scraping situation of an electrochemical probe by a blade, the relationship between the wall shear rate and the measurements of the mass transfer on the probe surface is not simple. It has been demonstrated that the use of an analytical solution corresponding to the quasi-steady state leads to erroneous values of the wall shear rate. This latter was then estimated either by analyzing the concentration field variations near the probe by taking into account the probe inertia as proposed by Sobolik et al. (1987), or by resolving the convective diffusion equation in the case of periodic flows. Yet, these wall shear rate estimations are to be validated. Accordingly, this paper is an attempt to accurately determine the wall shear rate on a mass transfer probe placed inside an SSHE by virtue of an inverse method.

2. MATERIALS AND METHODS

Electrodiffusional measurements have been carried out on a scale-down model of the Duprat TR 13x60 industrial exchanger. Geometrical characteristics of this industrial SSHE and its scale-down model are extensively described in Dumont et al. (2000a). The limiting diffusion current is measured on 0.4-mm-diameter circular microelectrodes embedded axially on the stator (Fig. 1b). The stainless-steel shaft serves as the counter-electrode and also as a reference electrode. The ferri-, ferrocyanide system ($Fe(CN_6)^{3-} + e^- \leftrightarrow Fe(CN_6)^{4-}$) is used with a large excess of supporting electrolyte K_2SO_4 so as to eliminate the migration current due to the electric field. Each experiment is carried out as follows: product flow rate (Q=35 $L.h^{-1}$), rotational speed of the rotor (N varied from 30 to 600 rpm) and product temperature (T=25°C) are adjusted to the desired values. For each rotational speed, the limiting diffusion current from the microelectrodes are numerically recorded up to 150s according to the flow regime.

In this study, the inverse mass transfer problem is applied from results obtained for three polymeric solutions: 1) a highly viscous Newtonian Emkarox HV45 – water solution (80/20, w/w). Emkarox HV45 (from ICI) is a mixture of polypropylene glycol and polyethylene glycol. The dynamic viscosity of this HV45 80/20 solution is η=1.18 Pa.s. 2) a low viscous Newtonian solution of polyethylene glycol 35000 (PEG; η=40 mPa.s). 3) a shear-thinning guar gum solution whose rheological behaviour was modelled by two different power-laws according to the shear rate domains: n=0.44 and k=6.40 $(Pa.s)^n$ for shear rate domain ranging from 2 to 20 s^{-1}; n=0.32 and k=8.91 $(Pa.s)^n$ for shear rate domain ranging from 10 to 1,234 s^{-1} (Dumont et al. 2000a).

The generalised Taylor number (Ta_g) is used to characterize the flow pattern. For HV45 and guar gum solutions, the maximum Ta_g value (obtained for the maximal rotational speed 600 rpm) is 11 and 34 respectively corresponding to laminar flow regime (see Dumont et al., 2000b), which is of main interest for applications at high fluid viscosities. For PEG solution maximum Ta_g value is 328.

The mass transfer diffusion number has been determined using the rotating electrode method (Levich, 1962) at T=25°C and it is given by the following table:

Table 1. Diffusion number of the different electrochemical solution at T=25°C

Electrochemical solution	HV45-80	PEG	Guar 1.2%
Diffusion number $m^2\ s^{-1}$	0.51 10^{-10}	3.5 10^{-10}	6.9 10^{-10}

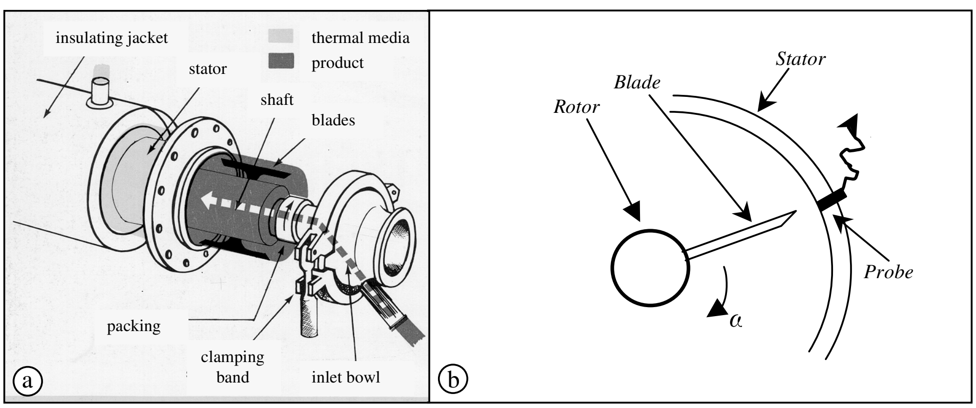

Figure 1. a) Principal design of SSHE (by courtesy of Duprat company) b) Schematic representation of a microelectrode embedded on outer cylinder

3. WALL SHEAR RATE CALCULATION AND INVERSE METHOD

The electrochemical method is based on the redox reaction on a surface of a probe mounted flush to an inert wall and the fluid. In this case, the mass transfer of the active ion in the flow near the probe surface is controlled by the convection-diffusion equation which is written in the viscous sub-layer for and at $Sc >> 1$ as follows:

$$\frac{\partial C}{\partial t} + S(t)Y\frac{\partial C}{\partial X} = D\left(\frac{\partial^2 C}{\partial X^2} + \frac{\partial^2 C}{\partial Y^2} + \frac{\partial^2 C}{\partial Z^2}\right) \tag{1}$$

where $C = C(X, Y, Z, t)$ is the concentration of the active ion in the flow, $S(t)$ is the wall shear rate, D is the diffusion coefficient, X is the mean flow direction and Y is the direction normal to the wall.

For a rectangular probe with a high aspect ratio (Length/width), the term $\frac{\partial^2 C}{\partial Z^2}$ is neglected and the equation (1) is written in a dimensionless form as follows:

$$f^+ \frac{\partial c}{\partial t^*} + S^*(t^*)y\frac{\partial c}{\partial x} = \overline{Pe}^{-\frac{2}{3}} \frac{\partial^2 c}{\partial x^2} + \frac{\partial^2 c}{\partial y^2} \tag{2}$$

where $t^* = f \cdot t$, $x = \frac{X}{l_e}$, $y = \frac{Y}{\delta_c}$, $c = \frac{C}{C_0}$, C_0 is the bulk concentration of the active ion, l_e is the probe width, $\delta_c = \left(\frac{l_e D}{\overline{S}}\right)^{\frac{1}{3}}$, $f^+ = f\frac{l_e^2}{D}\overline{Pe}^{-\frac{2}{3}}$, f is a characteristic flow frequency and $\overline{Pe} = \frac{\overline{S}\, l_e^2}{D}$ is the mean Peclet number.

The limiting diffusion current delivered by a single probe, may be presented in a dimensionless form as a Sherwood number $Sh(t)$ is defined as follows:

$$Sh(t) = \overline{Pe}^{\frac{1}{3}} \int_0^1 \left(\frac{\partial c}{\partial y}\right)_{y=0} dx \tag{3}$$

To calculate the wall shear rate from the limiting diffusion currents or the Sherwood delivered by every probe, many approaches can be found in the literature from what we notice in the quasi-steady solution law (Levêque, 1928). In the quasi-steady solution, the accumulation term of the mass transfer is not taken into consideration in the calculations ($f^+ \frac{\partial c}{\partial t^*} = 0$) which means that the probe is ideal (with no inertia). In this case and when the axial mass transfer diffusion term is negligible ($\overline{Pe}^{-2/3} \to 0$), the quasi-steady solution is written as follows:

$$S_q(t) = \frac{D}{l_e^2}\left(\frac{Sh(t)}{0.807}\right)^3 \tag{4}$$

In practice, $f^+ \neq 0$, the capacitive effect of the concentration sub-layer of the probe behaves as a non linear low pass filter, which delays the mass transfer response solution and attenuate its fluctuations rate in comparison with the ideal case (no inertia). This behavior of a real mass transfer probe induced many authors to correct the quasi-steady solution using Transfer functions method (Reiss and Hanratty (1962); Lebouché (1970); Fortuna and Hanratty (1971); Ambari et al. (1985); Nakoryakov et al.(1986); Deslouis et al. (1989, 1993); Geshev (1995)). Unfortunately, the use of the transfer function methods is limited to flows with low fluctuations rates and to measurements with moderate high frequency noise.

After examining the shortcomings of these latter, Sobolik et al. (1987) equally proposed an other method based on the correction of the wall shear rate, calculated from the Levêque quasi-steady solution $S_q(t)$, and corrected on the basis of the transient response of the probe.

The wall shear rate calculated by the Sobolik et al. (1987) method is given by the following expression:

$$S_c = S_q(t) + \frac{2}{3}\left(0.486 l_e^{\frac{2}{3}} D_e^{-\frac{1}{3}} S_q(t)^{-\frac{2}{3}}\right)\frac{\partial S_q(t)}{\partial t} \approx S_q(t) + 1.2045\frac{\partial S_q(t)}{\partial t} \tag{5}$$

This method proves to be well adapted than the transfer functions method for non reversing flows with important fluctuations, and this for high average Peclet numbers $\overline{Pe}$ (Rehimi et al., 2006). Altogether, the inverse method remains the only rigorous approach, despite its complexity. Hence, in the follow-up, we will compare only these two methods and the quasi-steady one $S_q(t)$.

3.1. Direct problem

The direct problem consists in developing a numerical tool able to simulate the response of a mass transfer probe to a wall shear rate excitation $S(t)$. By solving the equation (2), the probe response is calculated and written in a dimensionless form as $Sh(t)$ from equation (3).

The resolution of equation(2) is done numerically by the use of the finite volume method (Patankar, 1980). The computation domain is presented in the Fig.2 and divided into rectangular sub-volumes. The grid is chosen to take into consideration the evolution of the concentration values near the probe and to avoid an over meshing in the regions where the concentration evolution is not important. The boundary conditions are presented on the Fig.2. The algebraic system has been solved using Bi-conjugate gradient method stabilized (Bi-CGS) with an SSOR preconditioning (Markovic, 1995). After determining the concentration profile at the time t, the instantaneous Sherwood number $Sh(t)$ is obtained numerically by an integration of the equation (3) using Simpson method. For more details see Rehimi et al. (2006).

In the case of a circular probe of d_s diameter, the analogy proposed by Mitchell and Hanratty (1962) permits to consider the d_s diameter probe as a rectangular probe with an equivalent width $l_e = 0.82 d_s$. Certainly this approach is possible only when $\overline{Pe} \geq 1000$ to neglect the mass transfer diffusion in the span direction defined by the term $D\frac{\partial^2 C}{\partial Z^2}$ (Rehimi, 2006).

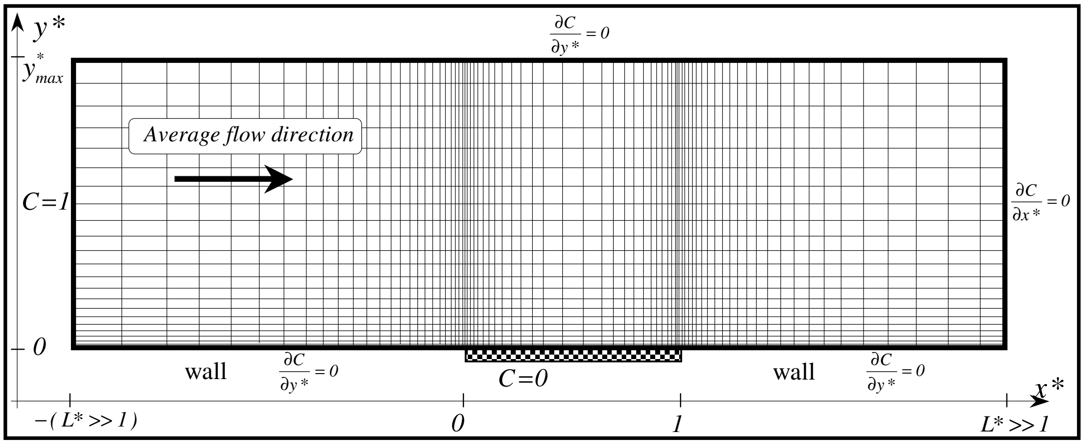

Figure 2. Boundary conditions and used grid for the calculation area

In order to verify the quality of the numerical solution obtained, validations are made first in steady regime by comparing the evolution of $Sh = f(Pe)$ obtained numerically with Levêque solution (1928) and the results of Geshev (1995). In unsteady regime, validations are made by comparing our transfer functions with those obtained by Ambari et al. (1985) and Deslouis et al. (1993). These results can be found in Rehimi et al. (2006) and in Rehimi (2006). Actually, it is important to estimate the accuracy of the results using these validations because they influence the estimation of the wall shear rate.

The validity and the quality of the obtained numerical solution are compared first in steady regime by plotting $Sh = f(Pe)$ and comparing it with the Levêque (1928) power law and the results proposed by Geshev (1995). Second, comparisons are made in dynamic regime between the numerical results and the transfer functions proposed by Ambari et al. (1986) and Deslouis et al. (1993). More details can be found in Rehimi et al. (2006) and Rehimi (2006).

3.2. Inverse problem and wall shear rate calculation

This step consists in introducing the direct problem as a routine in the minimization algorithm which permits (by comparing the experimental mass transfer $Sh_{exp}(t)$ and the numerical one $Sh_{num}(t)$) to estimate the real wall shear rate.

Let $\left(Sh_{\exp}(t_0^*), Sh_{\exp}(t_1^*), \Lambda\ , Sh_{\exp}(t_N^*)\right)$ the experimental mass transfer data delivered by a mass transfer probe under an excitation wall shear rate $\left(S^*{}_{exp}(t_0^*), S^*{}_{exp}(t_1^*), \Lambda\ , S^*{}_{exp}(t_N^*)\right)$.

The inverse method used, commonly known under the sequential estimation method or the function specification method, is based on the fact that one supposes that $S^*_{\exp}\left(t^* \le t^*_{k-1}\right)$ and $c\left(x, y, t^*_{k-1}\right)$ are known. In order to estimate $S^*_{\exp}(t_k^*)$, the idea consists in giving an acceptable first guess value $\hat{S}^*_{num}(t_k^*)$ of $S^*_{\exp}(t_k^*)$. This first guess $\hat{S}^*_{num}(t_k^*)$ is injected in the direct problem (Equation (2)) to calculate a first guess Sherwood number $\hat{Sh}_{num}(t_k^*)$. A Taylor series expansion truncated permits to define an updated guess $S^*_{num}(t_k^*)$ which is closer to $S^*_{exp}(t_k^*)$ as follow:

$$S^*_{num}\left(t^*_k\right) = \hat{S}^*_{num}\left(t^*_k\right) + \frac{\left(Sh_{exp}\left(t^*_k\right) - \hat{S}h_{num}\left(t^*_k\right)\right)}{\left(\dfrac{\partial \hat{S}h_{num}\left(t^*_k\right)}{\partial \hat{S}^*_{num}}\right)} \qquad (5)$$

where the quantity $\left(\dfrac{\partial \hat{S}h_{num}\left(t^*_k\right)}{\partial \hat{S}^*_{num}}\right)$ is calculated numerically.

The updated estimation $S^*_{num}\left(t^*_k\right)$ of $S^*_{exp}\left(t^*_k\right)$ is re-injected in the direct solution to obtain the updated values $c\left(x, y, t^*_k\right)$ and $Sh_{num}\left(t^*_k\right)$ and verifies:

$$\begin{cases} \left|Sh_{exp}\left(t^*_k\right) - Sh_{num}\left(t^*_k\right)\right| < \left|Sh_{exp}\left(t^*_k\right) - \hat{S}h_{num}\left(t^*_k\right)\right| \\ \left|Sh_{exp}\left(t^*_k\right) - Sh_{num}\left(t^*_k\right)\right| < \left|Sh_{exp}\left(t^*_{k-1}\right) - Sh_{num}\left(t^*_{k-1}\right)\right| \end{cases}$$

The time is then incremented and the previous operation is repeated at the time t^*_{k+1}.

In practice, the equation (5) is replaced by the following equation to give stability to the minimization algorithm:

$$S^*_{num}\left(t^*_k\right) = \hat{S}^*_{num}\left(t^*_k\right) + \frac{\sum_{m=1}^{r}\left(Sh_{exp}\left(t^*_{k+m}\right) - \hat{S}h_{num}\left(t^*_{k+m}\right)\right)\left(\dfrac{\partial \hat{S}h_{num}\left(t^*_{k+m}\right)}{\partial \hat{S}^*_{num}}\right)}{\sum_{m=1}^{r}\left(\dfrac{\partial \hat{S}h_{num}\left(t^*_{k+m}\right)}{\partial \hat{S}^*_{num}}\right)^2} \qquad (6)$$

where r is an integer as small as possible to avoid the apparition of a bias in the wall shear rate calculation.

The figure (3) resumes the wall shear rate estimation procedure.

4. RESULTS AND DISCUSSIONS

Numerical studies of fluids mechanics in a scraped surface heat exchanger with Newtonian and non-Newtonian fluids has been recently undertaken (Stranzinger et al., 2001; Sun et al., 2004). Stranzinger et al. (2001) omitted attachment of the scraper blades to the inner cylinder in the calculations. They showed that hydrodynamic pressure is primarily dominated by shear driven flow at Re>10 (due to inner cylinder rotation) while the pressure driven flow (due to the motion of the scraper blades) dominates for Re<10. These authors have demonstrated that the maximum shear stress appears at the scraping edge (outer cylinder) on the leading and trailing edges and reduces de 20% within a short distance. Likewise, Sun et al. (2004) showed for Newtonian fluids that shear rate is maximum close to the tip of the blades. For shear-thinning fluids, the "viscosity" is then reduced in these high shear regions.

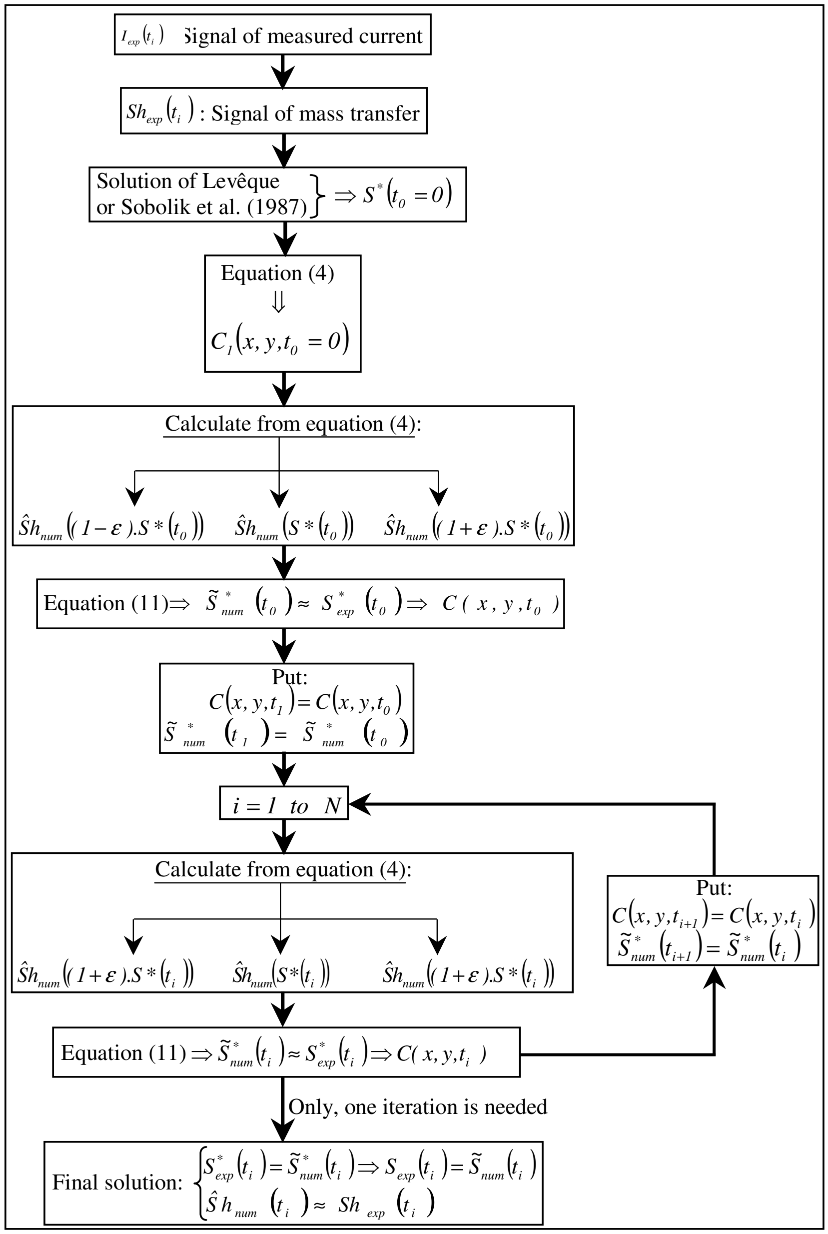

Figure 3. Inverse process for the determination of the wall shear stress from the measured instantaneous mass transfer

As previously demonstrated (Dumont et al., 2000b), high wall shear conditions occurs only when blades scrape the surface and depend on the gap between the edge of the blades and the outer wall surface. It is important to note that the increase of wall shear rates only occurs when the edge of the blade starts to scrape the probe. Before the probe is scraped, wall shear rates are only the results of the flow conditions; after scraping, caused perturbations are added.

The presence of high shear rate caused by blades at the wall surface are confirmed by Mabit et al. (2003). They experimentally observed high shear conditions on the leading edge of the blades. In this case, only a small quantity of product is affected by these high shear rates. Between scraping, shear rate remains low and quasi-constant. Numerical study developped by Stranzinger et al. (2001) agree with experimental results from Mabit et al. (2003). Stranzinger et al. (2001) showed that the flow phenomena in SSHE can be divided into two main parts. On the one hand, between the scraper blades, closed streamline loops are formed, which span the whole region between the blades. On the other hand, a "secondary flow exchange" takes place between the leading and the trailing edge of the scraper blades along the outer cylinder wall.

4.1. Mass transfer delivered by the probes

The figures 4.a,b,c represent examples of time evolutions of the Sherwood numbers for the three electrochemical solutions at different rotation frequencies of the blades. The Sherwood number is 2 N periodic since the SSHE contains two blades that give this periodic effect to the wall shear rate, and so to the mass transfer. The average mass transfer $\overline{Sh}$ in this case is an increasing function of the frequency of rotation N (Fig.5.a) which is the same in the absence of blades.

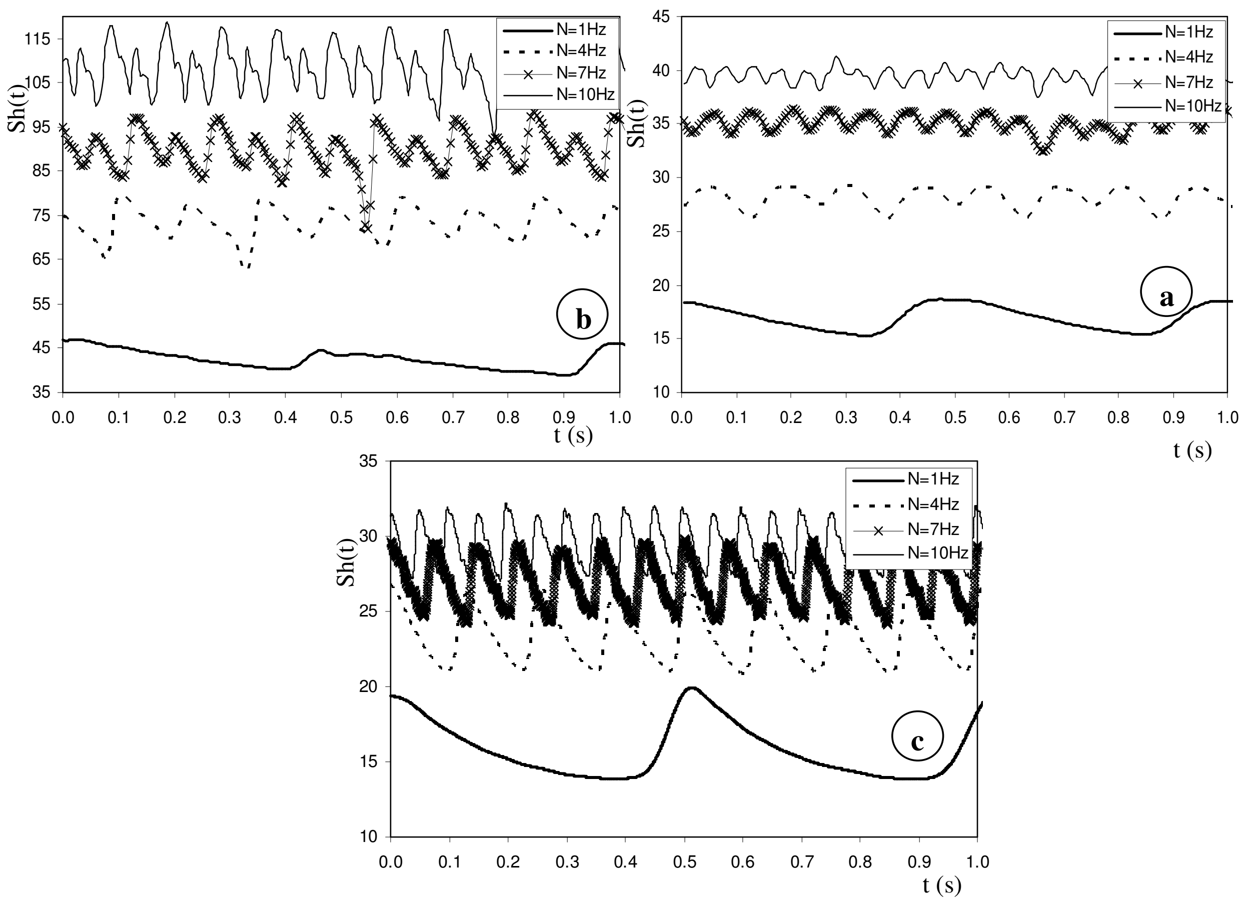

Figure 4. Time evolution of the Sherwood number for different rotation frequencies: a) PEG solution; b) HV-45 solution; c) Guar solution

The mass transfer fluctuations rate is a decreasing function of the rotation frequency N (Fig.5.b). This result is due to the probe response which behaves as a low pass filter. One should note that small fluctuations of the mass transfer do not imply low wall shear rate fluctuations, since the sensibility of the mass transfer probe depends on the flow regime and the dimensionless frequency f^+. The use of the transfer function methods, based on the linearization of the equation (2) for small wall shear rate fluctuations may inevitably lead to errors and will not be used for comparisons in the present.

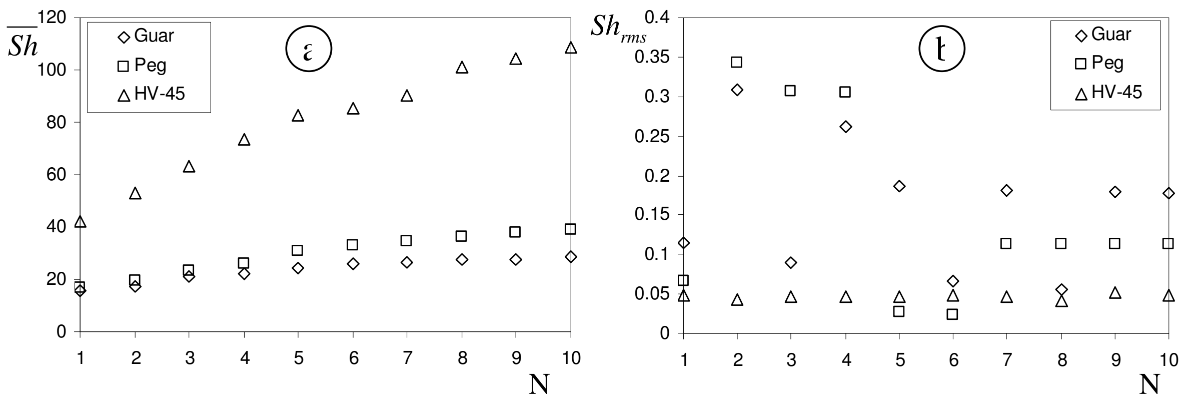

Figure 5. a) Evolution of the mean time Sherwood number for the different solution at different rotation frequencies; b) Evolution of the root mean square mass transfer for the different solutions at different rotation frequencies

4.2. Wall shear rate

The wall shear rates were calculated using Quasi-steady solution, Sobolik et al. (1987) method and inverse method with $r = 2$ in the equation (6). Results are given in the following figures (6, 7, and 8). As mentioned before, the non negligible capacitive effect of the electrochemical probe makes the quasi-steady solution become delayed and fluctuations attenuated in comparison with the real wall shear rate. The Sobolik et al. (1987) solution $S_{Sob}(t)$ and the inverse one $S_{Inv}(t)$ are sensibly identical. This result is predictable because the axial mass diffusion term is negligible ($\overline{Pe} > 7400$ for the Guar, $\overline{Pe} > 9200$ for the Peg and $\overline{Pe} > 1.4510^5$ for the HV-45). Nevertheless, one can notice the differences between $S_{Sob}(t)$ and $S_{Inv}(t)$ at extremum values of the wall shear rate. The difference consisting in $S_{Sob}(t) > S_{Inv}(t)$ at the maximum values of the wall shear rate is predictable because $S_{Sob}(t)$ is calculated on the assumption that the axial mass transfer diffusion term is negligible which gives the Sobolik et al. (1987) more sensitivity at the maximal values and does not give a correct behaviour in the wall shear rate calculation in a diffusion case or in a reversing flow case.

It is worth mentioning that the time evolutions of the wall shear rate given by the inverse method show in some cases a reversing flow just after the passing of a blade above the probe. Physically, a reversing flow after the passing of a blade can occur but this result must be confirmed using a sandwich or a tri-segment probe.

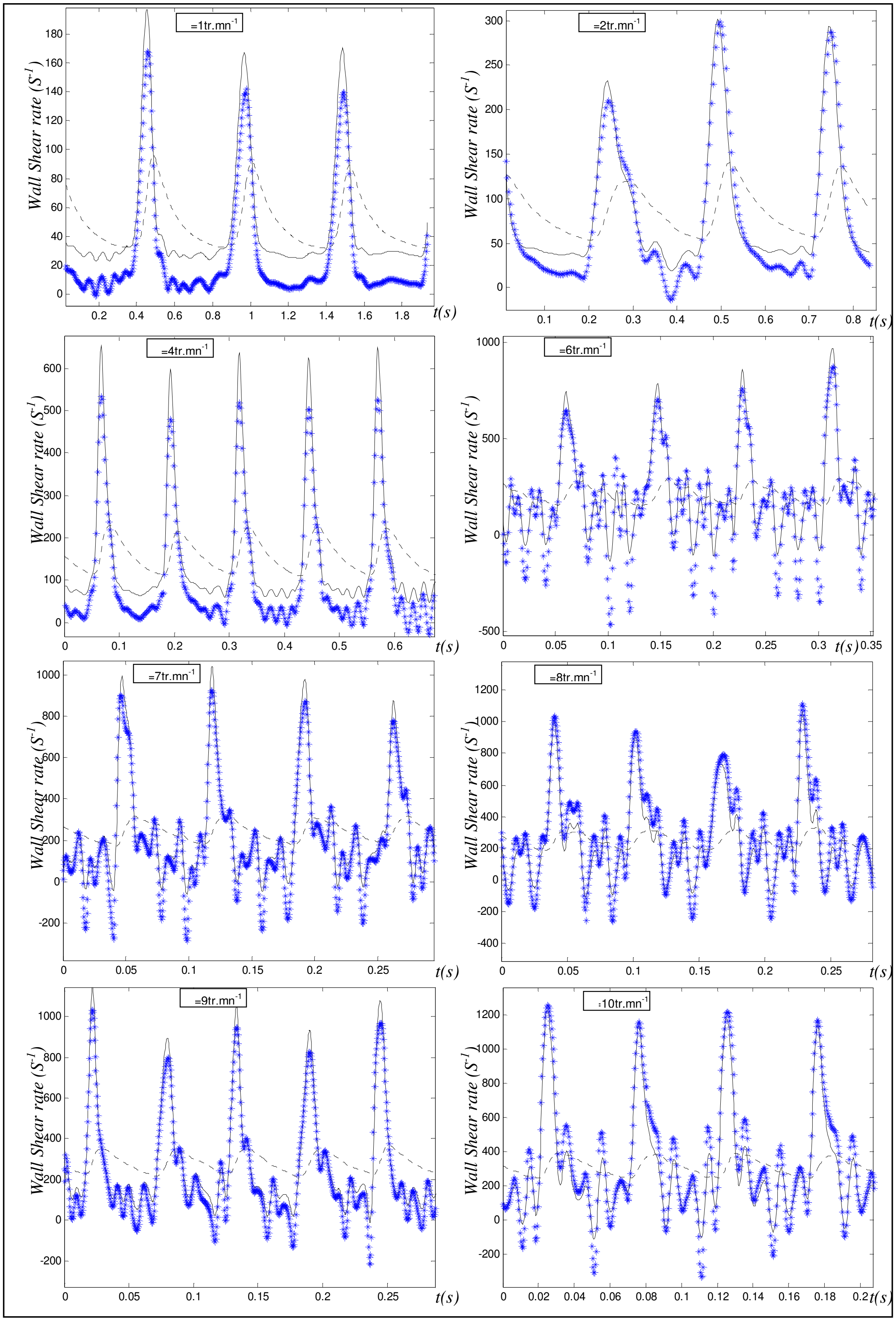

Figure 6. Wall shear rate for different rotation velocities of the blades for the Guar solution method blue stars; Sobolik method: continuous black; Quasi-steady solution: Dashed black

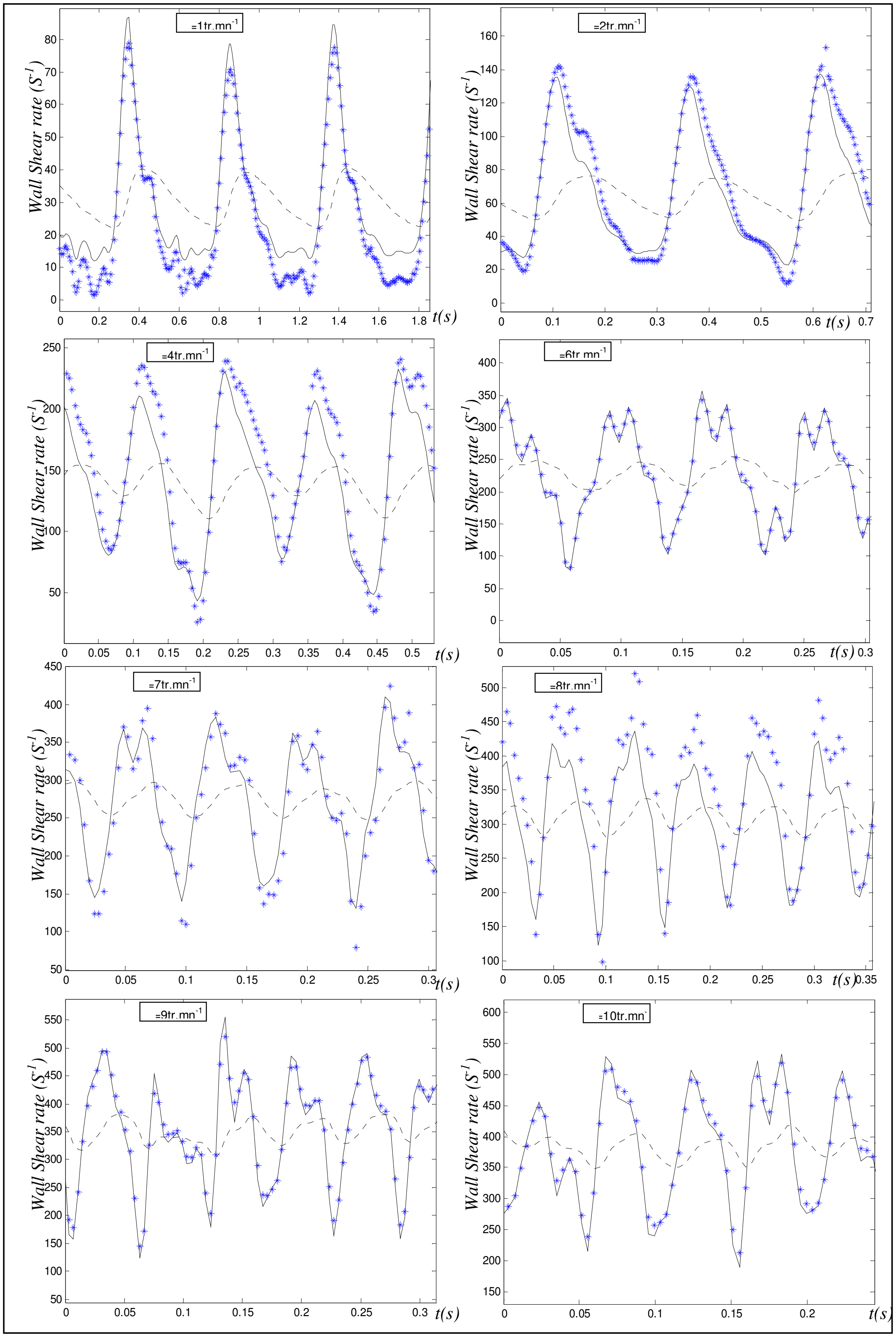

Figure 7. Wall shear rate for different rotation velocities of the blades for the PEG solution method blue stars; Sobolik method: continuous black; Quasi-steady solution: Dashed black

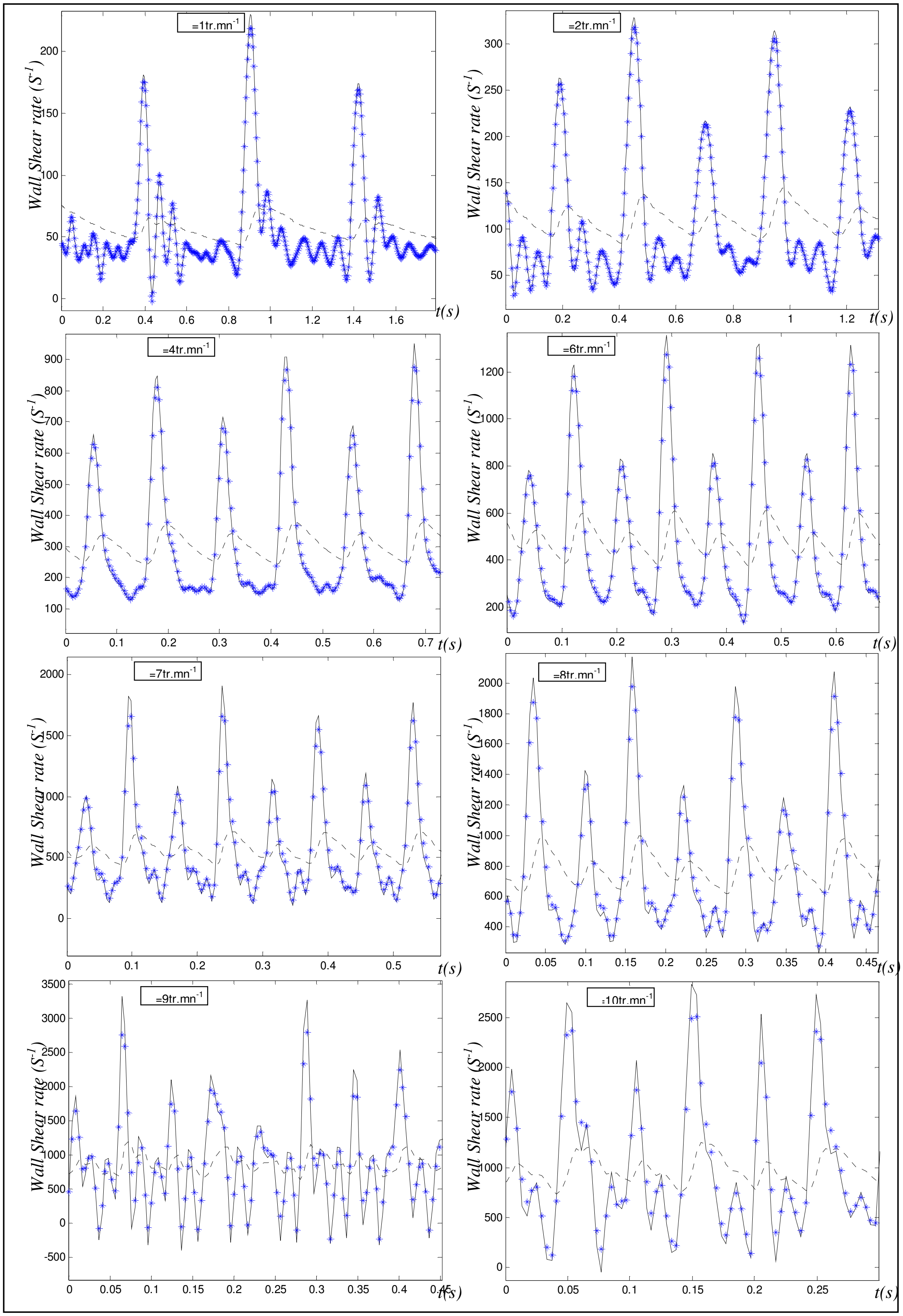

Figure 8. Wall shear rate for different rotation velocities of the blades for the HV-45 solution method blue stars; Sobolik method: continuous black; Quasi-steady solution: Dashed black

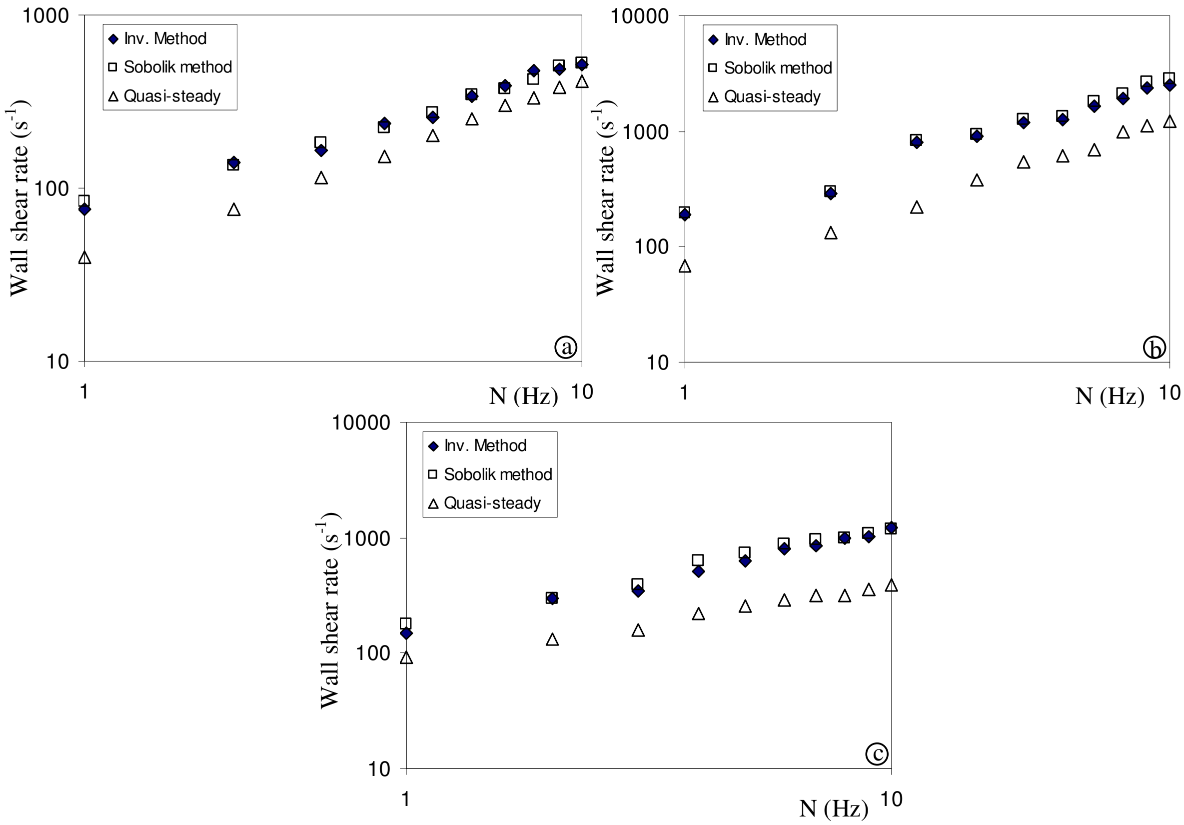

Figure 9. Maximal values of the wall shear rate in the SSHE at different rotation frequencies: a) PEG solution; b) HV-45 solution; c) Guar solution

In the SSHE, the calculation of the maximal values of the wall shear rate is capital for the quality of the products (especially in chemical of food engineering). The figures 9a, 9b and 9c show the evolution of the maximal values of the wall shear rate for the three solutions at different rotation frequencies. The gap between max ($S_{Sob}(t)$) and max ($S_{Inv}(t)$) remains for all the cases less than 10%, which remains acceptable in comparisons with other methods. This result confirm the idea that consists in using the Sobolik et al. (1987) as a rapid and quantitatively acceptable method for the wall shear rate calculation when the flow is two dimensional, non reversal and at high mean Peclet numbers. This assumption is confirmed by the inverse method.

5. CONCLUSIONS

In this work, the wall shear rate is studied inside a scraped surface heat exchanger for three different electrochemical solutions. The wall shear rate was calculated using three methods: quasi-steady solution, Sobolik et al. (1987) solution and the inverse method (sequential estimation). Independently of the fluid nature (Newtonian or not), the quasi-steady solution does not reflect the reality, especially in the maximum values of the wall shear rate which is obtained on the probe surface when the blades pass above it. Using the inverse method, the wall shear rate is accurately calculated.

Since (in the present work) the axial mass transfer diffusion terms are negligible, the wall shear rate may be rapidly obtained using the Sobolik et al. (1987) method with 10% accuracy.

References

1. A. Ambari, C. Deslouis, B. Tribollet, *Int. J. Heat Mass Transfer* 29 (1985) 35
2. C. Deslouis, O. Gil, B. Tribollet, *J. Fluid Mech.*, 215 (1989) 85
3. C. Deslouis, F. Huet, O. Gil, B. Tribollet, *Experiments in Fluids*, 16 (1993) 97
4. E. Dumont, F. Fayolle, J. Legrand, *AIChE J.*, 46(6) (2000a) 1138
5. E. Dumont, F. Fayolle, J. Legrand, *J. Food. Eng.*, 45, (2000b) 195
6. P. I. Geshev, *J. Electroanalytical Chemistry*, 410 (1995) 1
7. G. S. Jeremy, A modern frame work for high performance linear algebra, Master Thesis, University of Notre Dame, Department of Computer Science and Engineering, Indiana, (1999).
8. K. Kataoka, H. Doi, T. Komai, *Int. J. Heat Mass Transfer*, 20(1977) 57
9. J. Legrand, F. Coeuret , M. Billon, *Int. J. Heat Mass Transfer*, 26 (1983) 1075
10. M. A. Levêque, *Ann. Mines*, 13 (1928) 381
11. J. Mabit, F. Fayolle, J. Legrand, *Chem. Eng. Sci.*, 58 (2003)4667
12. S. V. Patankar, Numerical Heat transfer fluid flow, Hemisphere/ Mc Graw-Hill, New York, 1980.
13. A. Markovic, An investigation of sparse matrix solvers with applications to models of transport in porous media, Master in sciences, Center in statistical science and industrial mathematics, Queensland University of Technology, (1995).
14. V. E. Nakoryakov, A. P. Budukov, O. N. Kashinsky, P. I. Geshev, Electrodiffusion method of investigation into local structures of turbulent flows, (ed. Gasenko V. G.) Novosibirsk (1986).
15. F. Rehimi, F. Aloui, S. Ben Nasrallah, L. Doubliez, J. Legrand, *Int. J. of Heat and Mass Transfer*, 49 (2006) 1242
16. L. P. Reiss, T. J. Hanratty, *A.I.Ch.E Journal*, 9 (1963) 154
17. V. O. Sobolik, J. O. Wein, J. Cermak, *Collection Czechoslovak Cem. Commun.*, 52(1987) 913
18. M. Stranzinger, K. Feigl K, E. Windhab, *Chem. Eng. Sci.*, 56 (2001) 3347
19. K. –H. Sun, D. L. Pyle, A. D. Fitt , C. P. Please, M. J. Baines, N. Hall-Taylor N., *Computers & Fluids*, 33 (2004) 869
20. S. Wronski, M. Jastrzebski, *Rheologica Acta*, 29 (1990) 453